

Wireless Link Statistical Bit Error Model

John J. Lemmon



U.S. DEPARTMENT OF COMMERCE
Donald L. Evans, Secretary

Nancy J. Victory, Assistant Secretary
for Communications and Information

June 2002

This Page Intentionally Left Blank

This Page Intentionally Left Blank

Product Disclaimer

Certain commercial equipment, instruments, or materials are identified in this report to specify the technical aspects of the reported results. In no case does such identification imply recommendation or endorsement by the National Telecommunications and Information Administration, nor does it imply that the material or equipment identified is necessarily the best available for the purpose.

This Page Intentionally Left Blank

This Page Intentionally Left Blank

CONTENTS

	Page
FIGURES	vi
ABSTRACT	1
1. INTRODUCTION	1
2. THE MODEL	2
3. PROBABILITIES	3
4. PARAMETER ESTIMATION	6
5. LAND MOBILE RADIO LINK PERFORMANCE	8
6. WIRELESS LOCAL AREA NETWORK PERFORMANCE	22
7. CONCLUSIONS AND RECOMMENDATIONS FOR FURTHER WORK	25
8. ACKNOWLEDGMENTS	26
9. REFERENCES	26

FIGURES

		Page
Figure 1.	Transition diagram and bit error probabilities for the Gilbert model.	3
Figure 2.	Land mobile radio system performance relating BER to SNR and parametrically to ISR.	10
Figure 3.	Transition probability q versus SNR for the land mobile radio link simulations. Each curve corresponds to a different value of ISR.	11
Figure 4.	Transition probability Q versus SNR for the land mobile radio link simulations. Each curve corresponds to a different value of ISR.	12
Figure 5.	Probability h of transmitting a bit correctly (in the B state) versus SNR for the land mobile radio link simulations. Each curve corresponds to a different value of ISR.	12
Figure 6.	Comparison of error burst length distributions generated by (a) waveform simulation and (b) the Gilbert model for an “average” land mobile radio link.	14
Figure 7.	Comparison of error gap length distributions generated by (a) waveform simulation and (b) the Gilbert model for an “average” land mobile radio link.	15
Figure 8.	Comparison of error burst length distributions generated by (a) waveform simulation and (b) the Gilbert model for a FSFL land mobile radio link.	16
Figure 9.	Comparison of error gap length distributions generated by (a) waveform simulation and (b) the Gilbert model for a FSFL land mobile radio link.	17
Figure 10.	Comparison of error burst length distributions generated by (a) waveform simulation and (b) the Gilbert model for an IL land mobile radio link.	18
Figure 11.	Comparison of error gap length distributions generated by (a) waveform simulation and (b) the Gilbert model for an IL land mobile radio link.	19

Figure 12.	Comparison of error burst length distributions generated by (a) waveform simulation and (b) the Gilbert model for a NL land mobile radio link.	20
Figure 13.	Comparison of error gap length distributions generated by (a) waveform simulation and (b) the Gilbert model for a NL land mobile radio link.	21
Figure 14.	Plot of the analytic representation of the error gap length distribution in the Gilbert model for an “average” land mobile radio link.	22
Figure 15.	Wireless local area network performance relating BER to SNR.	23
Figure 16.	Gilbert model parameters q , Q , and h versus SNR for the wireless local area network link simulations.	24
Figure 17.	Error burst length distributions generated by a waveform simulation and by the Gilbert model for a wireless local area network with SNR = 12 dB and CIR = 10 dB.	24
Figure 18.	Error gap length distributions generated by a waveform simulation and by the Gilbert model for a wireless local area network with SNR = 12 dB and CIR = 10 dB.	25

This Page Intentionally Left Blank

This Page Intentionally Left Blank

WIRELESS LINK STATISTICAL BIT ERROR MODEL

John J. Lemmon¹

A bit error model that enables simulations of the digital error performance of wireless communication links has been developed. The model development has been based on error sequences derived from waveform simulations of wireless link performance with various modems operating under varying propagation, noise, and interference conditions. Values of the model parameters are obtained by analyzing the distributions of the lengths of error bursts and error gaps (error-free intervals). Mathematical expressions have been derived for the means and variances of the error burst and error gap distributions of the model as functions of the model parameters. Constraining the means and variances to the values obtained from waveform simulations uniquely determines values of the model parameters corresponding to a given set of link conditions. Examples of error burst and error gap distributions obtained from waveform simulations are compared with those generated by the model for a land mobile radio system and a wireless local area network. The simulated and model distributions are quite similar; however, the model runs tens of thousands of times faster than the corresponding waveform simulations, enabling rapid determination of link performance.

Keywords: wireless communication link, bit error model, Markov chain, waveform simulation

1. INTRODUCTION

The Institute for Telecommunication Sciences (ITS) is currently collaborating with the National Institute of Standards and Technology (NIST) to develop national information infrastructure research and evaluation capabilities. One area of this project, the wireless communications performance benchmarking program, includes the development of a statistical bit error model serving as a demonstration of technology that could be used in higher level network simulations.

Wireless network performance simulation depends on knowledge of the statistical distribution of bit errors for each wireless link represented in the network. The distribution is a function of all the link variables, including the channel, noise, interference, modem, coding, equalization, etc. The bit errors encountered on a communication link can be obtained by a waveform level simulation of the entire link. However, this kind of simulation can be computationally prohibitive, particularly for simulations of networks comprising many links.

¹The author is with the Institute for Telecommunication Sciences, National Telecommunications and Information Administration, U.S. Department of Commerce, Boulder, CO 80305.

A more efficient form of simulation is discrete event simulation, whereby one generates a bit error stream directly. Waveform simulation typically uses many samples per bit and requires simulating the entire communication link for each sample. By contrast, discrete event simulation of bit errors requires only one sample per bit, and, as will be seen, only requires the generation of one or two random numbers per sample.

ITS has undertaken the development of a wireless link bit error model that enables discrete event simulation of the bit errors encountered on wireless links. The model development has been based on error streams derived from waveform simulations of link performance under various conditions. Values of the model parameters have been determined by analyzing the distributions of the lengths of error bursts and error gaps (error-free intervals). It will be shown that the distributions generated by the waveform simulations and by the model are quite similar; however, the calculations with the statistical model typically run tens of thousands of times faster than the waveform simulations (the precise increase in speed depends on the type of link being simulated).

Section 2 of this report presents the statistical model. Expressions for the error burst and error gap length distributions are derived in Section 3 and are used to relate the model parameters to measurable quantities, as discussed in Section 4. In Sections 5 and 6 the model is compared with waveform simulations of the digital performance of land mobile radio systems and wireless local area networks under various conditions. Concluding remarks and recommendations for additional work are made in Section 7.

2. THE MODEL

Bit error models generate a sequence of noise bits (where zeros represent good bits and ones represent bit errors) that is modulo 2 added to input bits to produce output bits. Models can be grouped into two broad classes: memoryless models and those with memory. In memoryless models the noise bits are produced by a sequence of independent trials. Each trial has the same probability $P(0)$ of producing a correct bit and probability $P(1) = 1 - P(0)$ of producing a bit error.

Measured data from actual communication links indicate that many links have memory, that is, the errors occur in isolated bursts. This is because many link impairments, such as impulsive noise, switching transients, and multipath fades, are bursty in nature. A commonly used technique to endow a model with memory is to make the bit error probability depend on the states of a Markov chain.

The use of Markov chains in bit error models was initiated by Gilbert [1]. The Gilbert model is based on a Markov chain with two states: G (for good) and B (for bad or for burst). In state G, transmission is error-free. In state B, the link has probability h of transmitting a bit correctly. A transition diagram and bit error probabilities for the Markov chain are shown in Figure 1. For suitably small values of the transition probabilities $p = \text{Prob}(B \rightarrow G)$ and $P = \text{Prob}(G \rightarrow B)$, the states B and G tend to persist and the model simulates bursts of errors.

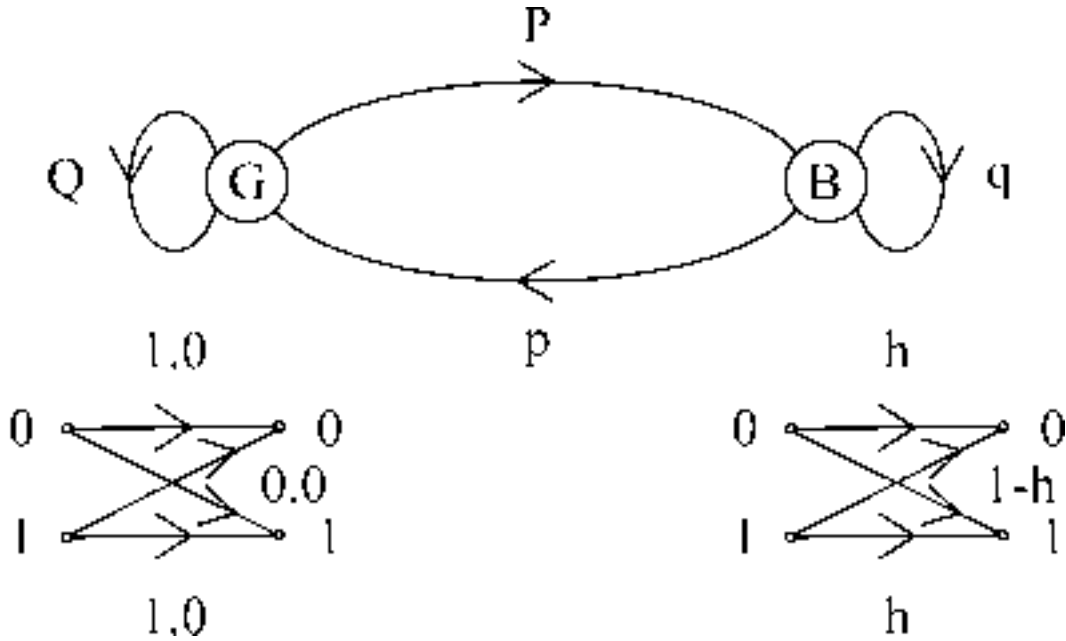


Figure 1. Transition diagram and bit error probabilities for the Gilbert model.

This simple model has three independent parameters (p , P , and h) and was originally used to describe performance measurements over telephone circuits. Whether the model is adequate to describe the error performance of wireless links has been investigated in the present work. One can envisage more complicated models with more parameters (e.g., more than two states in the Markov chain); however, determination of the model parameters from measured data becomes more difficult as the number of parameters increases.

3. PROBABILITIES

The parameters p , P , and h are not directly observable and must therefore be determined from statistical measurements of the error process. Runs of G alternate with runs of B . The run lengths have geometric distributions, with mean $1/P$ for the G -runs and $1/p$ for the B -runs. The fraction of time spent in state B is therefore $P(B) = P/(P+p)$. Since bit errors occur only in state B , and with probability $1-h$, the probability of error is

$$P(1) = (1-h)P(B) = (1-h)\frac{P}{p+P}. \quad (1)$$

The sequence of states cannot be reconstructed from the sequence of bits in the error process, because both zeros and ones (good bits and bit errors) are produced in the B state. Thus, the distributions of run lengths of the states cannot be used to determine the model parameters from measurements of the error process. However, the bits of the error process itself, (i.e., runs of

zeros and ones) are observable, and the distributions of run lengths of zeros (error gaps) and ones (error bursts) can be used to determine the model parameters.

An expression for the error burst length distribution can be derived as follows. Error bursts can only occur in the B state. Therefore, given the occurrence of a one, the probability that the next $K-1$ bits are ones is $q^{K-1}(1-h)^{K-1}$, where $q = 1-p$. After a run of K ones, the error burst can terminate in either of two ways: the random process can return to the G state, the probability for which is $p = q-1$, or it can remain in the B state and produce a zero, the probability for which is qh . Thus, the probability distribution for error bursts of length K , defined as the conditional probability that, given a zero followed by a one, the next $K-1$ bits are ones followed by a zero, is

$$P(1^{K-1}0|01) = q^{K-1}(1-h)^{K-1}[1-q(1-h)], \quad K=1,2,\dots \quad (2)$$

The notation 1^{K-1} denotes a run of $K-1$ ones.

Error gaps can occur in either the B state or the G state, and the derivation of an expression for the distribution of error gap lengths is therefore less straightforward than that for the error burst lengths. However, Gilbert [1] has shown how recurrent events theory can be used to obtain the needed probabilities. Let f_k denote the conditional probability that, given state B, the next return to B will occur at step K :

$$f_K = P(G^{K-1}B|B). \quad (3)$$

Then $f_1 = q$, $f_2 = pP$, and $f_k = pQ^{k-2}P$ for $K \geq 2$, where $Q = 1-P$. These probabilities can be viewed as the coefficients of a generating function $F(t)$ of recurrence time probabilities:

$$F(t) = \sum_{K=1}^{\infty} f_K t^K = qt + \frac{pPt^2}{1-Qt}. \quad (4)$$

The probability $f_k^{(m)}$ that the m th return to B happens at step K has the generating function

$$\sum_{K=1}^{\infty} f_k^{(m)} t^K = [F(t)]^m. \quad (5)$$

Starting from a one (and hence from state B), the next one must occur at a return to B. The probability that, given the occurrence of a one, the next one will occur on the m th return to B at step K is

$$h^{m-1}(1-h) f_K^{(m)}. \quad (6)$$

It follows that, given a one, the probability that the next one will occur at step K (regardless of the number of returns to B) is

$$v(K-1) = P(0^{K-1}1|1) = \sum_{m=1}^{\infty} h^{m-1}(1-h) f_K^{(m)}. \quad (7)$$

Multiplying (7) by t^K , summing over K , and making use of (5) leads to the generating function $V(t) = \sum v(K)t^K$:

$$tV(t) = \frac{(1-h)F(t)}{1-hF(t)}. \quad (8)$$

Substituting (4) into (8),

$$V(t) = \frac{(1-h)[q + (p-Q)t]}{D(t)}, \quad (9)$$

where $D(t) = 1 - (Q+hq)t - h(p-Q)t^2$.

Now factor the quadratic $D(t)$:

$$D(t) = (1-Jt)(1-Lt), \quad (10)$$

where

$$2J = Q + hq + \sqrt{(Q+hq)^2 + 4h(p-Q)}, \quad (11)$$

and L is given by the same expression with a negative square root. Substituting (11) into (9), $V(t)$ becomes

$$V(t) = \frac{(1-h)[q + (p-Q)t]}{J-L} \left(\frac{J}{1-Jt} - \frac{L}{1-Lt} \right). \quad (12)$$

The coefficient of t^K in the power series expansion of $V(t)$ is

$$v(K) = \frac{1-h}{J-L} [(qJ + p-Q)J^K - (qL + p-Q)L^K]. \quad (13)$$

A recurrence formula for $v(K)$ can be found by writing (9) as $D(t)V(t) = (1-h)[q+(p-Q)t]$ and equating coefficients of t^K :

$$v(K) = (Q + hq)v(K-1) + h(p-Q)v(K-2), \quad K=2,3,\dots \quad (14)$$

Initial values are

$$v(0) = (1-h)q, \quad v(1) = (1-h)(pP + hq^2). \quad (15)$$

The probability distribution for error gaps of length K , defined as the conditional probability that, given the occurrence of a one followed by a zero, the next $K-1$ bits are zeros followed by a one, is

$$P(0^{K-1}1|10) = \frac{v(K)}{1-v(0)}, \quad K=1,2,3,\dots \quad (16)$$

Substitution into (16) of either (13) or (14) and (15) leads to the error gap length distribution as a function of the model parameters.

4. PARAMETER ESTIMATION

The determination of the three parameters p , P , and h from measurements of the error process requires that the parameters be expressed as functions of three other parameters that are directly observable. Clearly, many parameters exist that could be used for this purpose. For example, Gilbert [1] used the probability of error $P(1)$ and the conditional probabilities $P(11)/[P(10)+P(11)]$ and $P(111)/[P(101)+P(111)]$.

The purpose of the present work has been to develop a model that can be used to simulate the error process and correctly reproduce all of its statistical properties. To validate the model, the error processes generated by the model must be compared to measured error processes. Since these processes consist of alternating runs of zeros and ones, the processes can be characterized by the probability distributions of the lengths of error bursts (runs of ones) and error gaps (runs of zeros). From this point of view, the objective of the parameter estimation is to choose values of the model parameters that generate error burst and error gap distributions that resemble the corresponding measured distributions as closely as possible. For this reason the parameter estimation has been formulated in terms of the error burst and error gap distributions.

The first and second moments (means and variances) of the measured distributions can be used to determine the model parameters as follows. Use of the identity

$$\sum_{K=1}^{\infty} Kx^{K-1} = \frac{d}{dx} \sum_{K=0}^{\infty} x^K = \frac{1}{(1-x)^2}, \quad |x| < 1 \quad (17)$$

enables one to calculate the mean error burst length μ_{EB} from (2),

$$\mu_{EB} = \frac{1}{1 - q(1 - h)}, \quad (18)$$

and the mean error gap length μ_{EG} from (13) and (16),

$$\mu_{EG} = \frac{h(1 - Q) + (1 - q)}{(1 - h)(1 - Q)[1 - q(1 - h)]}. \quad (19)$$

Similarly, the identity

$$\sum_{K=1}^{\infty} K^2 x^{K-1} = \frac{d}{dx} \left(x \frac{d}{dx} \sum_{K=0}^{\infty} x^K \right) = \frac{1+x}{(1-x)^3}, \quad |x| < 1 \quad (20)$$

in conjunction with (2), (13), and (16) implies that the variance σ_{EB}^2 of the error burst distribution is

$$\sigma_{EB}^2 = \frac{\sqrt{q(1-h)}}{1 - q(1-h)} \quad (21)$$

and the variance σ_{EG}^2 of the error gap distribution is

$$\sigma_{EG}^2 = \left[\frac{1-h}{[1 - q(1-h)](J-L)} \left(\frac{(qJ+p-Q)J(J+1)}{(1-J)^3} \right) \right] + [J+L] - \mu_{EG}^2. \quad (22)$$

Note that the functional relationships in (18) and (21) involve only two of the model parameters, q and h , in the combination $q(1-h)$. Therefore, these two relationships are not independent and cannot be used to simultaneously determine values of q and h ; each relationship determines a value of the quantity $q(1-h)$, and these values are likely to be different if the measured error burst lengths do not have a geometric distribution. To avoid this difficulty, (21) has not been used in the parameter determination. Instead, (18), (19), and (22), which provide three independent functions of the model parameters, have been used to simultaneously determine values of the three parameters.

Using (18) and (19) to solve for Q and h in terms of q , μ_{EB} , and μ_{EG} , one finds

$$1 - h = \left(1 - \frac{1}{\mu_{EB}} \right) \frac{1}{q} \quad (23)$$

and

$$P = 1 - Q = \frac{1 - q}{\left(1 + \frac{\mu_{EG}}{\mu_{EB}}\right) \left(1 - \frac{1}{\mu_{EB}}\right) \frac{1}{q} - 1}. \quad (24)$$

Substitution of (23) and (24) into (22) results in a relationship between q and the measured quantities σ_{EG}^2 , μ_{EB} , and μ_{EG} . This relationship is evaluated numerically and a value of q determined. Substitution of this value of q into (23) and (24) determines values of h and $P=1-Q$, respectively. In this way values of the model parameters have been determined for a variety of link conditions.

Note that using μ_{EB} and μ_{EG} to determine the model parameters guarantees that the model will generate the measured bit error probability, because the measured means determine the error probability through the relationship

$$P(1) = \frac{\mu_{EB}}{\mu_{EB} + \mu_{EG}}. \quad (25)$$

As a consistency check, substitution of (18) and (19) into (25) yields the expression in (1) for $P(1)$.

5. LAND MOBILE RADIO LINK PERFORMANCE

The viability of the statistical model to simulate the digital performance of wireless links has been investigated by comparing the bit error processes generated by the statistical model and by waveform simulations for a variety of land mobile radio link conditions. Error burst and error gap length distributions have been derived from the waveform simulations and used to determine values of the model parameters for various link conditions. The dependence of the model parameters on link conditions has been investigated to demonstrate that well-defined relationships exist between the link conditions and the model parameters. Finally, these parameter values have been used in the model to generate error burst and error gap length distributions to be compared with those generated by the waveform simulations.

5.1 Waveform Simulations

The waveform simulations were performed with a commercial communication link simulation tool that was enhanced with additional modules developed at ITS. This tool enables the user to configure a communication link with modular transmitter, channel, and receiver models, and has been used to simulate the performance of a variety of wireless links, as described by Quincy and Achatz [2].

Three types of channel distortion were used in the simulations: time-varying multipath, additive noise, and interference. The simulations illustrate the performance of a binary frequency shift keying (BFSK) mobile system operating at a frequency of 900 MHz and traveling through an urban canyon. The source is random data at a rate of 14.4 kbps.

The propagation model of the urban canyon, based on measurements by Cox [3], uses three independent, time-varying propagation paths separated by delays. The first path is not delayed and is, on average, the strongest path. The second path is delayed by 5 μ s and has an average power 8 dB below that of the first path. The third path is delayed by 8 μ s and has an average power 15 dB below that of the first path. Doppler shifts as high as 80 Hz are possible in any of the paths. The amplitude and phase of each path are controlled by a time-varying Jakes model.

After the transmitted signal is distorted by the propagation channel, noise and interference are added to the received signal. Receiver front-end noise is modeled as additive white Gaussian noise. Cochannel interference is modeled by a transmitter also operating with BFSK modulation at 14.4 kbps.

Simulations were performed with signal-to-noise ratios (SNR) that varied from 0 to 50 dB in steps of 10 dB and interference-to-signal ratios (ISR) that varied from 0 to -40 dB in steps of 10 dB. The simulations varied in length, depending on the error performance. Each simulation was run in blocks of 5000 bits until a minimum of 1500 errors occurred.

Figure 2 shows the bit-error-rate (BER) plotted versus the SNR. Each curve corresponds to a different value of the ISR. As expected, the BER increases with increasing ISR and decreasing SNR. From these curves, three limiting cases of performance can be identified: (1) noise limited (NL), (2) interference limited (IL), and (3) frequency selective fading limited (FSFL). In the NL case an increase in SNR decreases the BER. In the IL case, a change in the ISR dramatically affects the BER for the same SNR. In the FSFL case, the interference is minimal and performance is not improved by increasing the SNR; the frequency selective fading, caused by multipath, is limiting the performance.

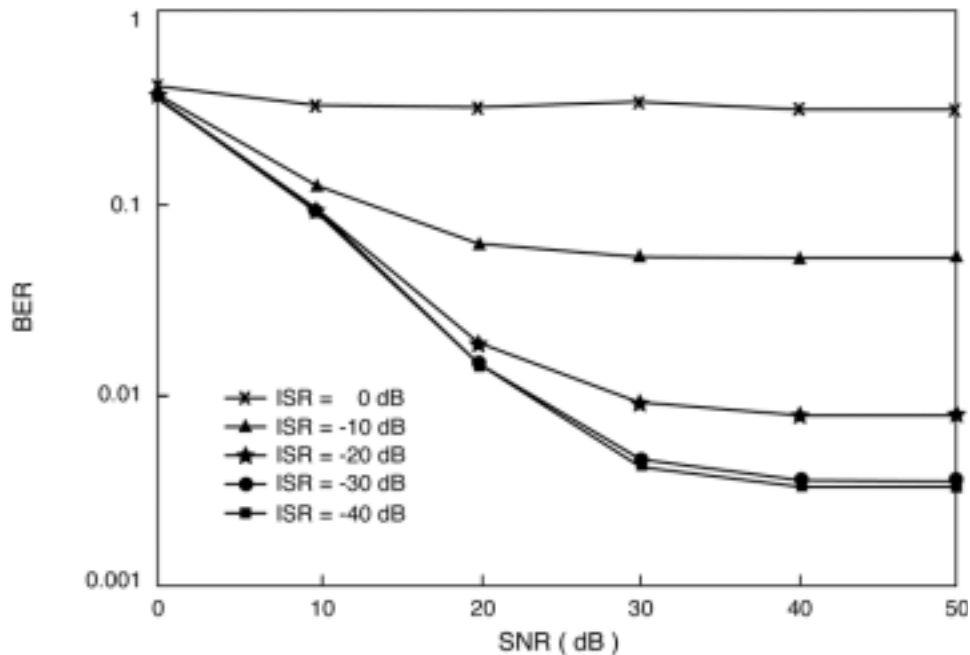


Figure 2. Land mobile radio system performance relating BER to SNR and parametrically to ISR.

5.2 Dependence of Model Parameters on Link Conditions

For each waveform simulation, the error gap length and error burst length distributions were generated and values of the model parameters determined, as described in Section 4. The results for q , Q , and h are shown in Figures 3, 4, and 5, respectively. Like the BER curves in Figure 2, each parameter is plotted versus the SNR, and each curve corresponds to a different value of the ISR.

The results in Figure 3 indicate that q decreases with increasing SNR and decreasing ISR (i.e., decreasing BER). This is consistent with heuristic expectations, because one expects the Markov chain to spend less time lingering in the bad state as the error probability decreases.

Conversely, the curves in Figure 4 show that Q increases with increasing SNR and decreasing ISR (except at the lowest value of SNR). Thus, the Markov chain tends to spend more time lingering in the good state as the error probability decreases.

The results in Figure 5 seem less amenable to heuristic interpretation, since they indicate that the variations in h are not monotonic in either SNR or ISR. However, at the lower values of SNR, h tends to increase with increasing SNR and decreasing ISR, as one would expect (probability of a correct bit in the bad state increases as the error probability decreases).

Heuristic interpretations aside, what is important about these results is that the parameters vary in a smooth, deterministic fashion with varying link conditions (SNR and ISR). A meaningful correspondence therefore exists between the model parameters and the link conditions. The determination of analytic expressions for these relationships via empirical curve fitting has not been carried out. However, such expressions would provide a useful tool for evaluating the model parameters for given link conditions, without having to carry out waveform simulations and statistical measurements of the bit error process or interpolations between the parameter values shown in Figures 3-5.

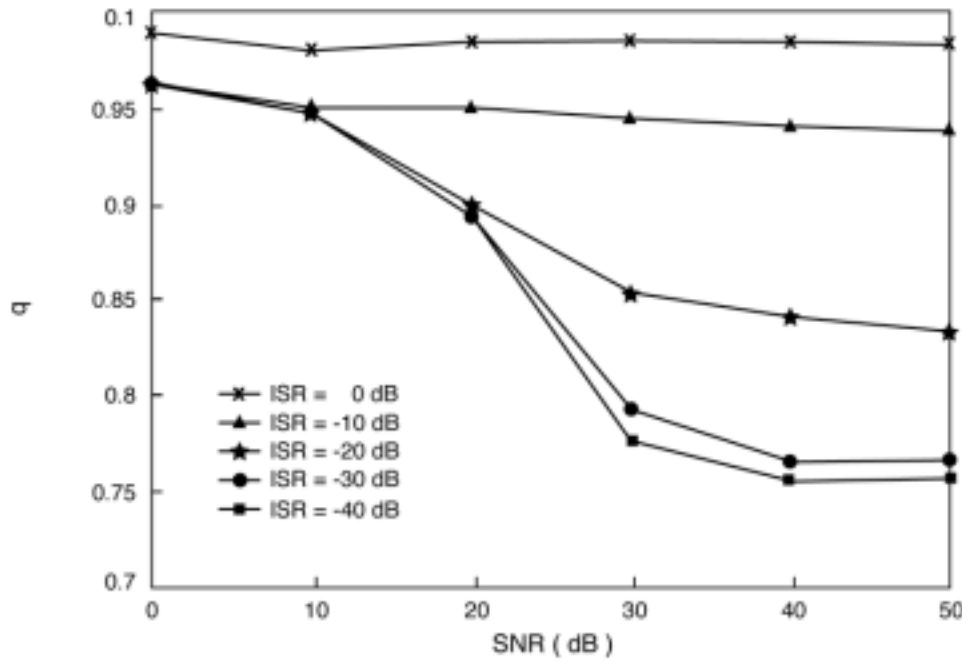


Figure 3. Transition probability q versus SNR for the land mobile radio link simulations. Each curve corresponds to a different value of ISR.

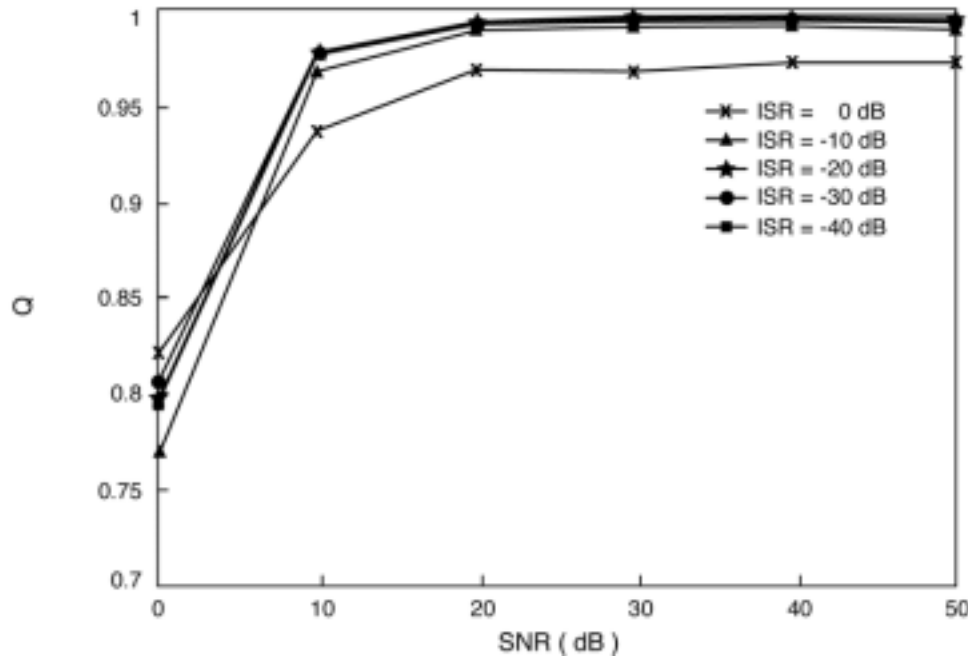


Figure 4. Transition probability Q versus SNR for the land mobile radio link simulations. Each curve corresponds to a different value of ISR.

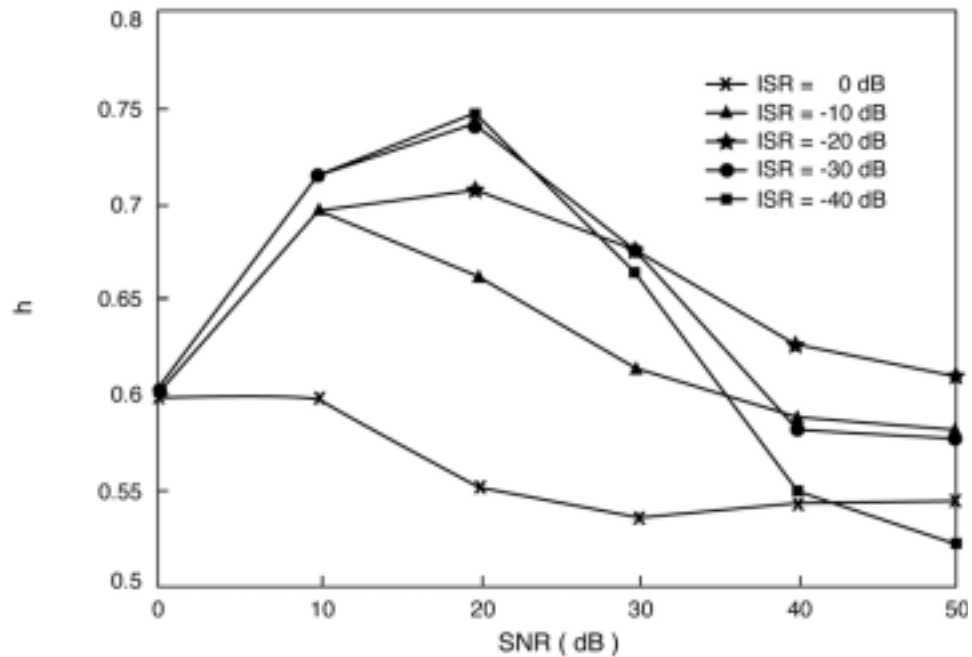


Figure 5. Probability h of transmitting a bit correctly (in the B state) versus SNR for the land mobile radio link simulations. Each curve corresponds to a different value of ISR.

5.3 Comparison of Model with Waveform Simulations

Having determined values of the model parameters, it remains to show that the model correctly reproduces the characteristics of the error process. To this end, the model was used to generate error processes for an NL link (SNR=10 dB, ISR=-40 dB), an IL link (SNR=50 dB, ISR=-10 dB), an FSFL link (SNR=50 dB, ISR=-40 dB), and an “average” link (SNR=30 dB, ISR=-20 dB). The lengths of the simulations using the model are the same as those of the corresponding waveform simulations. It was found that the model runs approximately 50,000 times faster than the waveform simulations.

Comparisons of the error burst length and error gap length distributions generated by the model with those generated by the waveform simulations for these four cases are shown in Figures 6-13. In each figure the probability that an error burst or error gap is of a given length is plotted versus that length (in bits) in the form of a histogram. The vertical scale in the error gap distributions has been made logarithmic to more clearly reveal the long tail in the distributions at large error gap lengths.

The distributions generated by the statistical model and by the waveform simulations show generally good agreement with the exception of one feature in the error gap distributions: the distributions generated by the waveform simulations have a local minimum at gap lengths in the vicinity of 25 followed by a slight bump in the distributions at gap lengths in the vicinity of 75. The apparent absence of this feature in the error gap distributions generated by the model cannot be attributed to statistical noise in the distributions due to the finite length of the simulations, because the analytical expression (13) for the error gap distribution in the statistical model does not have this feature. As an illustration of this, Figure 14 shows the error gap distribution for the “average” link computed with the recurrence formula given by (14)-(16) and clearly indicates that this feature is absent. This relatively minor feature could perhaps be simulated by generalizing the model; for example, the number of states could be increased. However, this has not been investigated due to the increased complexity it would add to the model.

Quantitative comparisons of the distributions generated by the model and by the waveform simulations are difficult, because analytical expressions for the distributions generated by the waveform simulations, analogous to those for the model, do not exist. Thus, any measure of disagreement would largely reflect the statistical noise in the distributions generated by the waveform simulations, which could only be eliminated by running simulations with excessively long computation times.

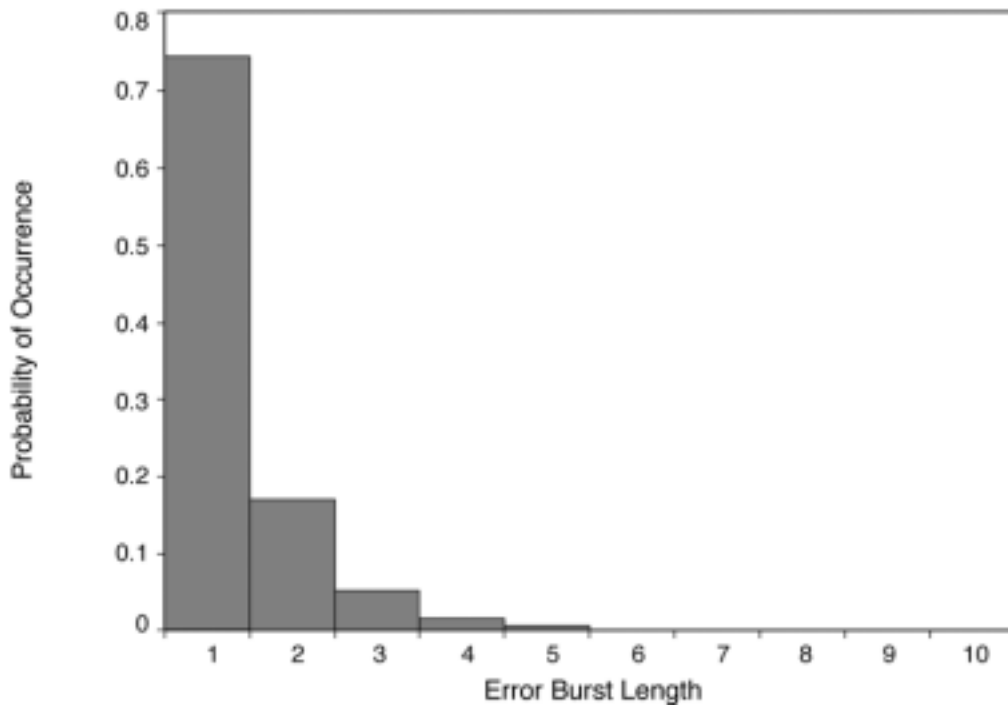
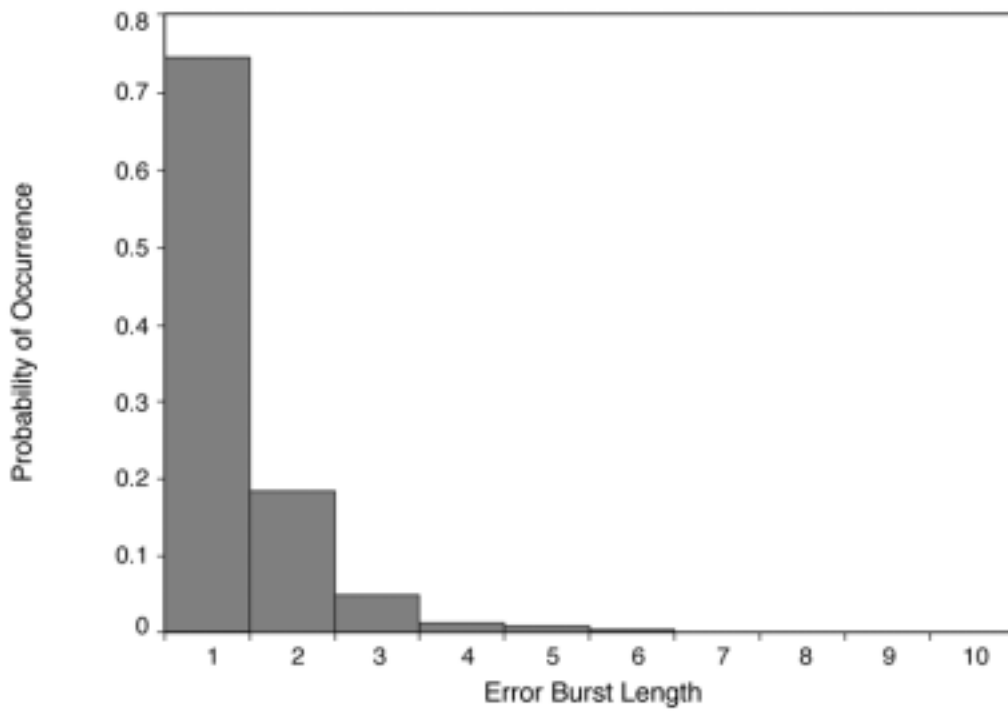


Figure 6. Comparison of error burst length distributions generated by (a) waveform simulation and (b) the Gilbert model for an "average" land mobile radio link.

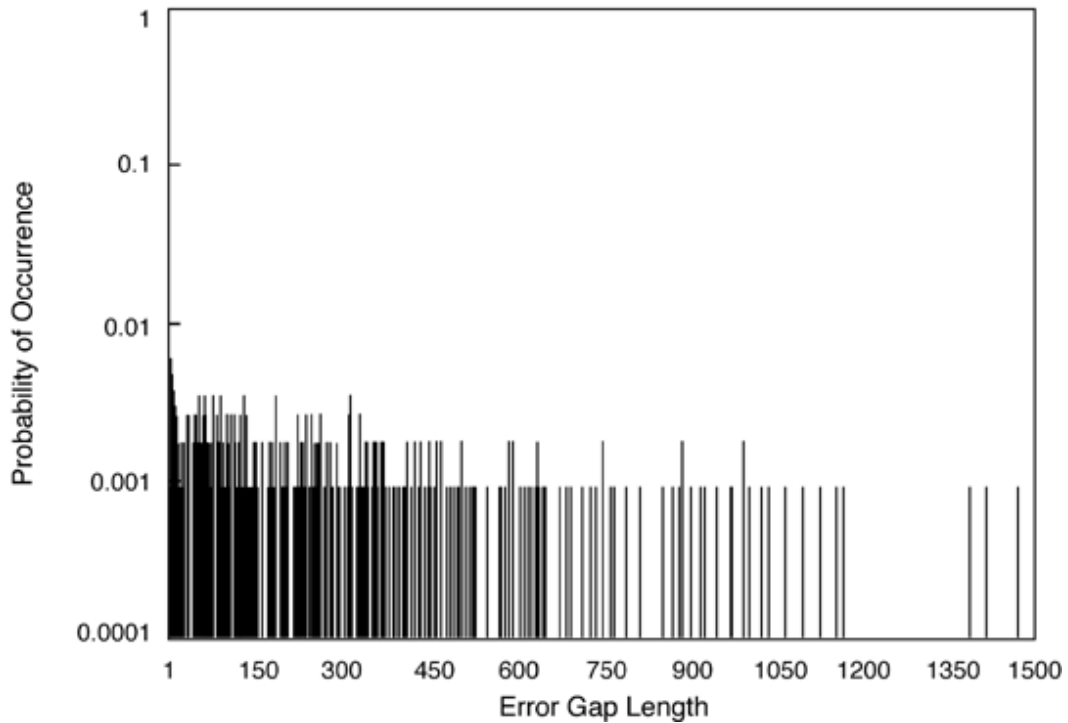
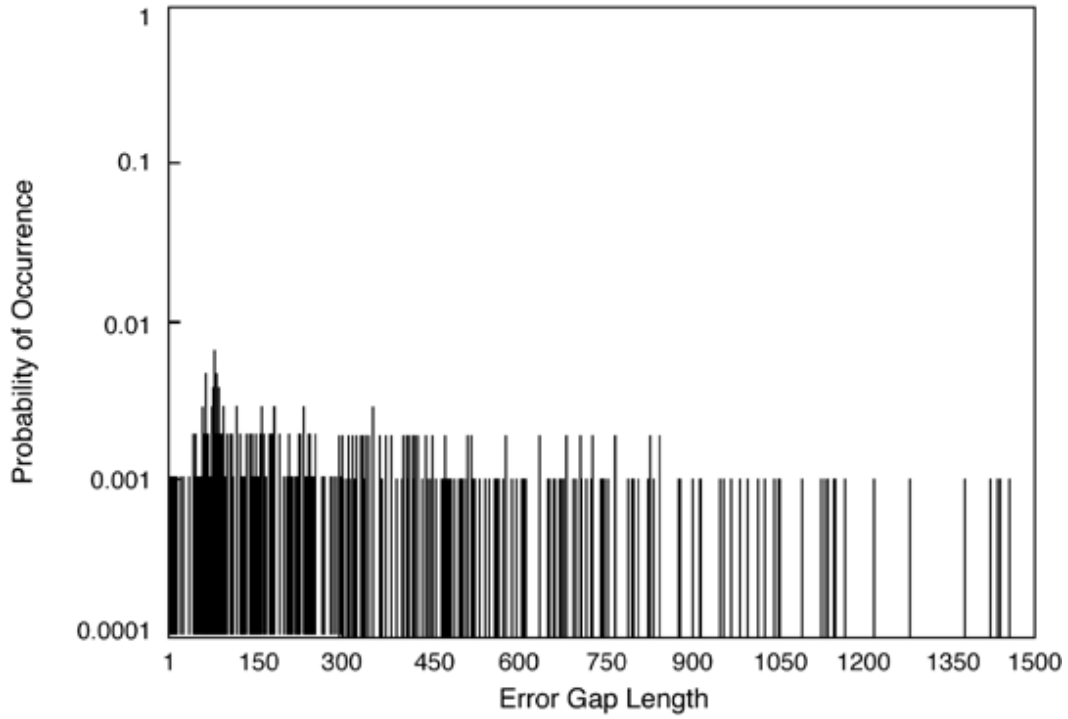


Figure 7. Comparison of error gap length distributions generated by (a) waveform simulation and (b) the Gilbert model for an "average" land mobile radio link.

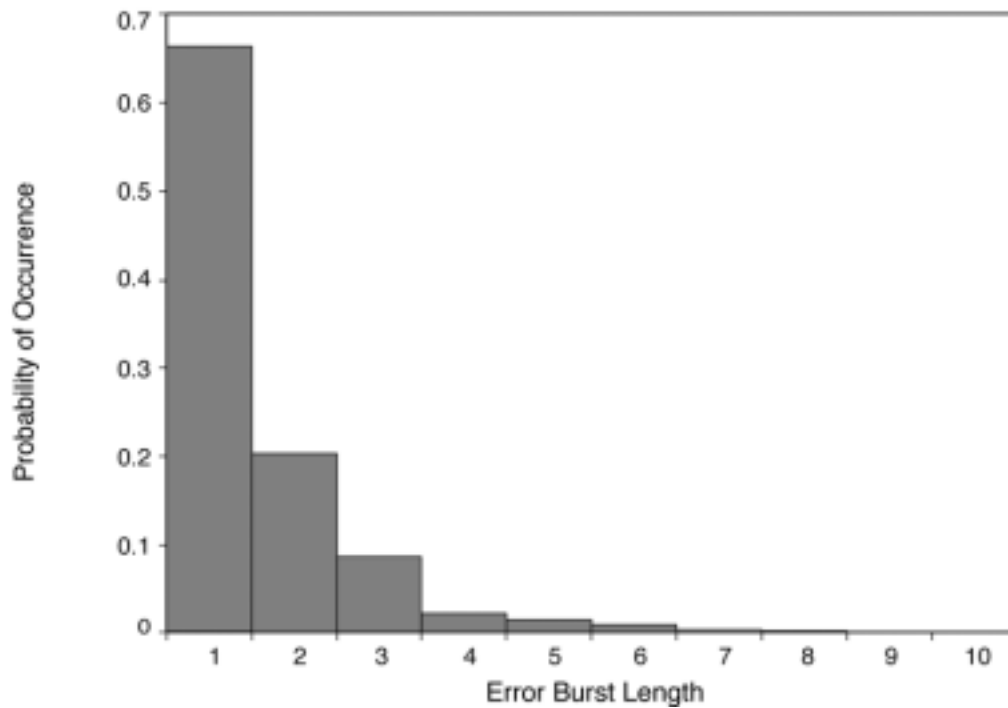
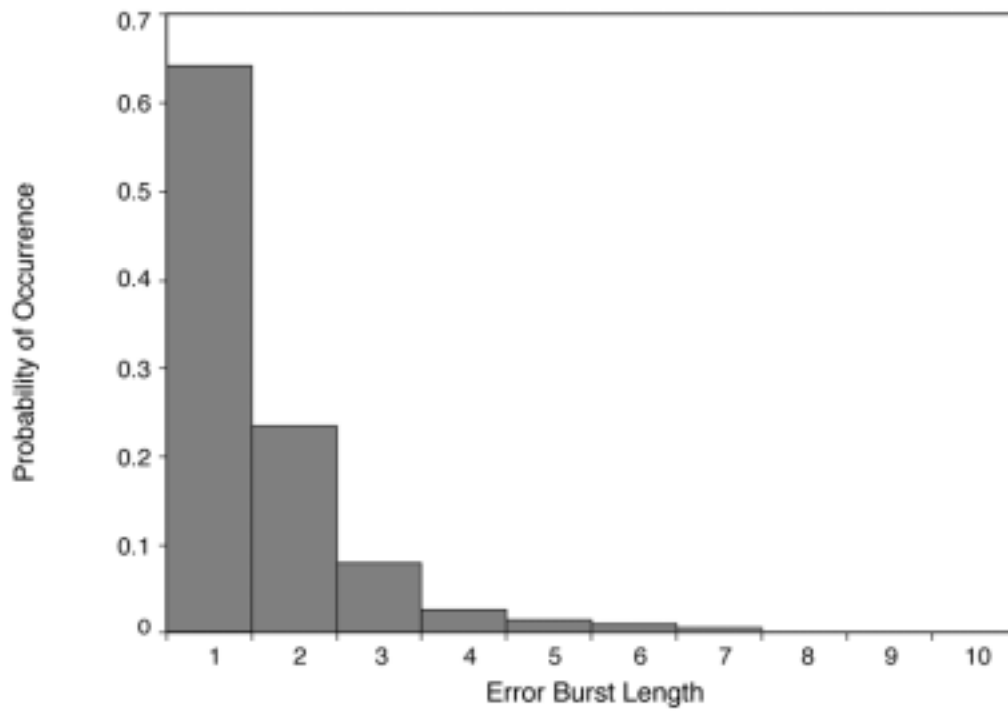


Figure 8. Comparison of error burst length distributions generated by (a) waveform simulation and (b) the Gilbert model for a FSFL land mobile radio link.

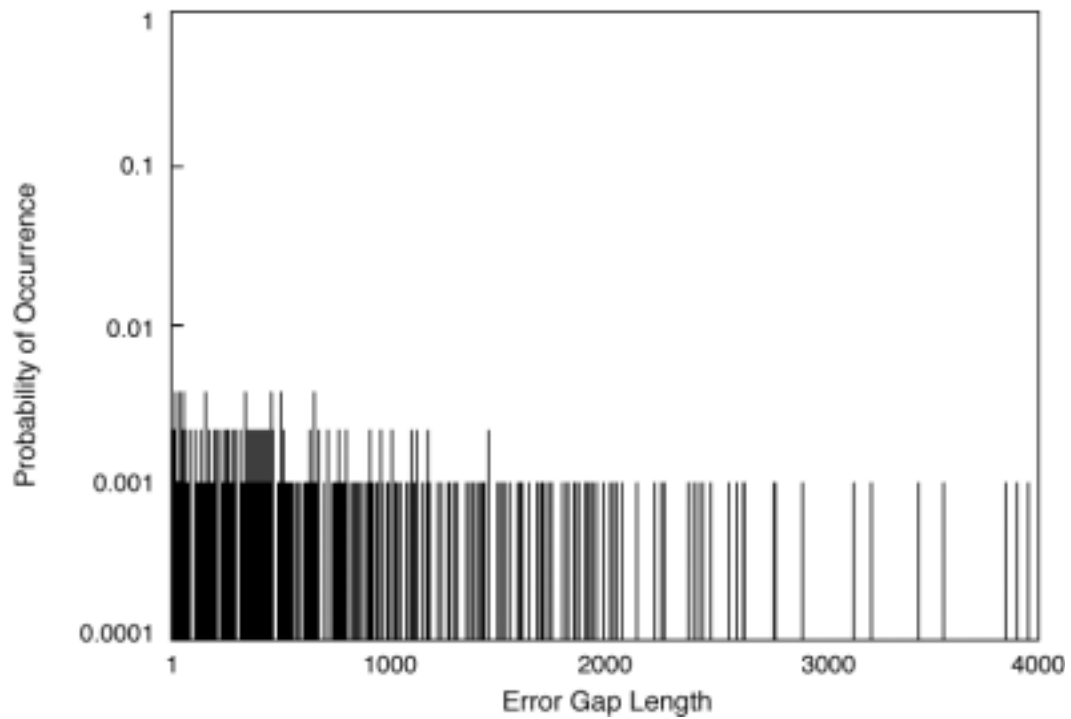
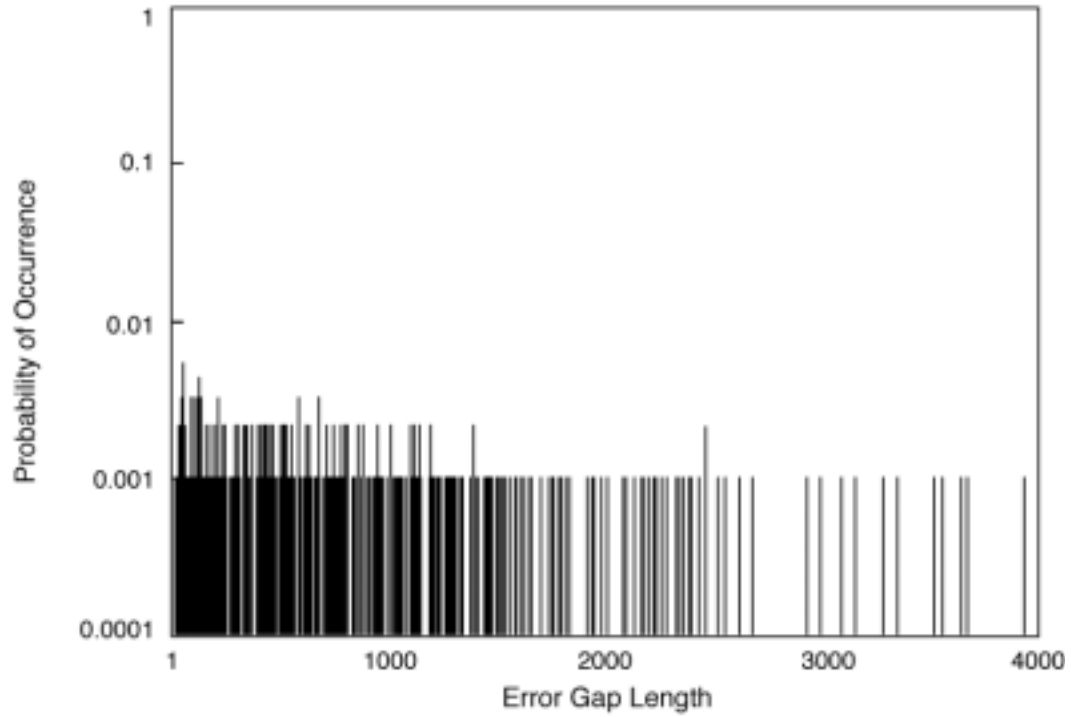


Figure 9. Comparison of error gap length distributions generated by (a) waveform simulation and (b) the Gilbert model for a FSFL land mobile radio link.

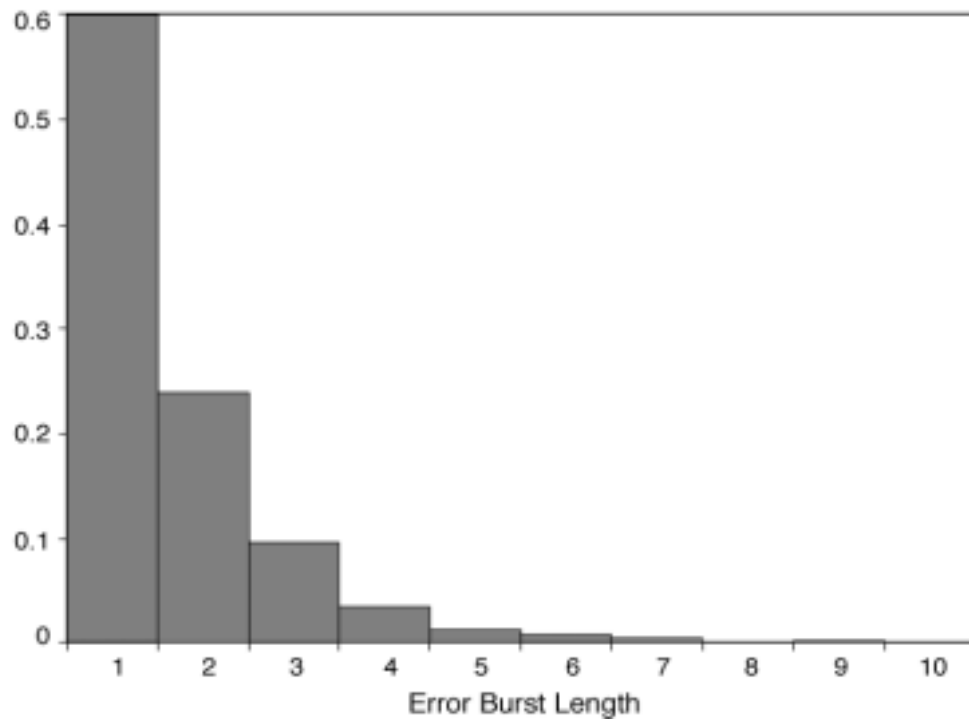
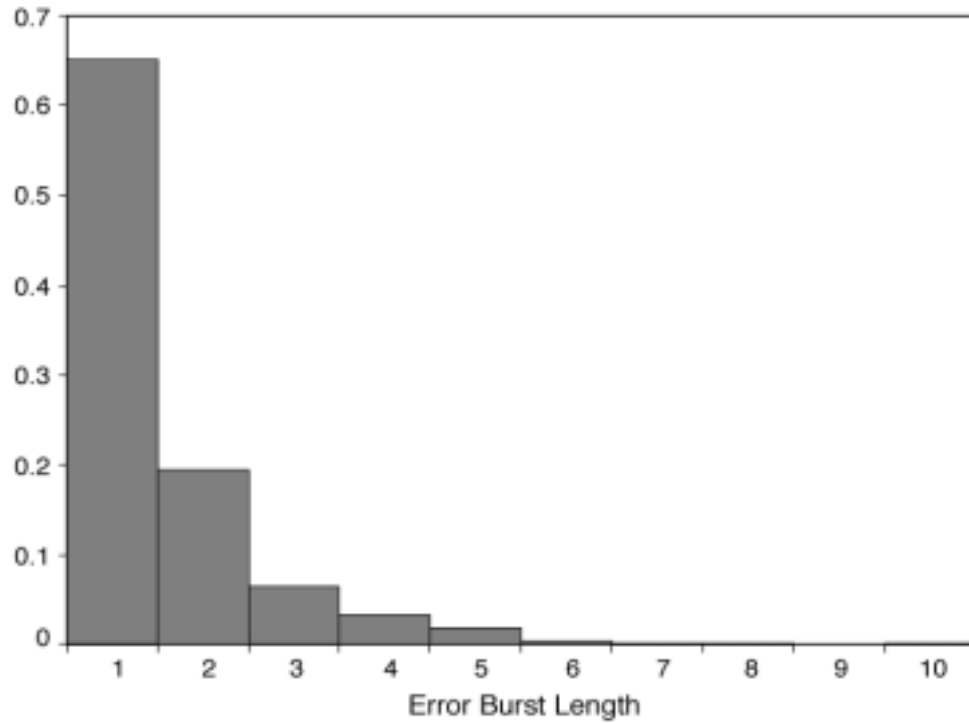


Figure 10. Comparison of error burst length distributions generated by (a) waveform simulation and (b) the Gilbert model for an IL land mobile radio link.

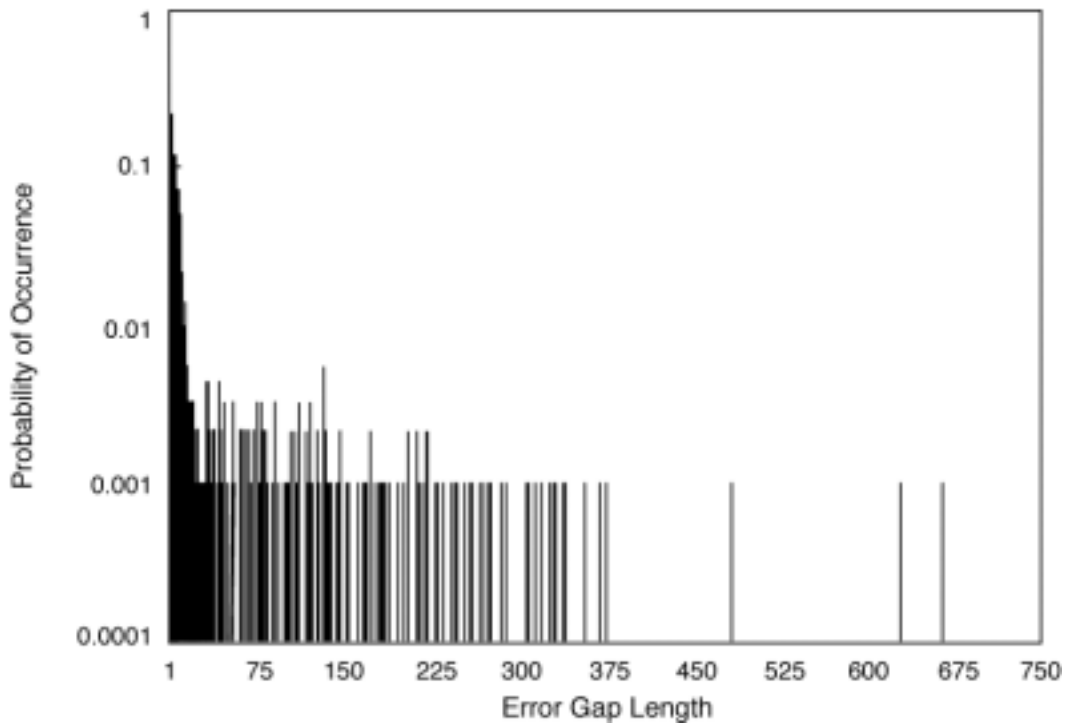
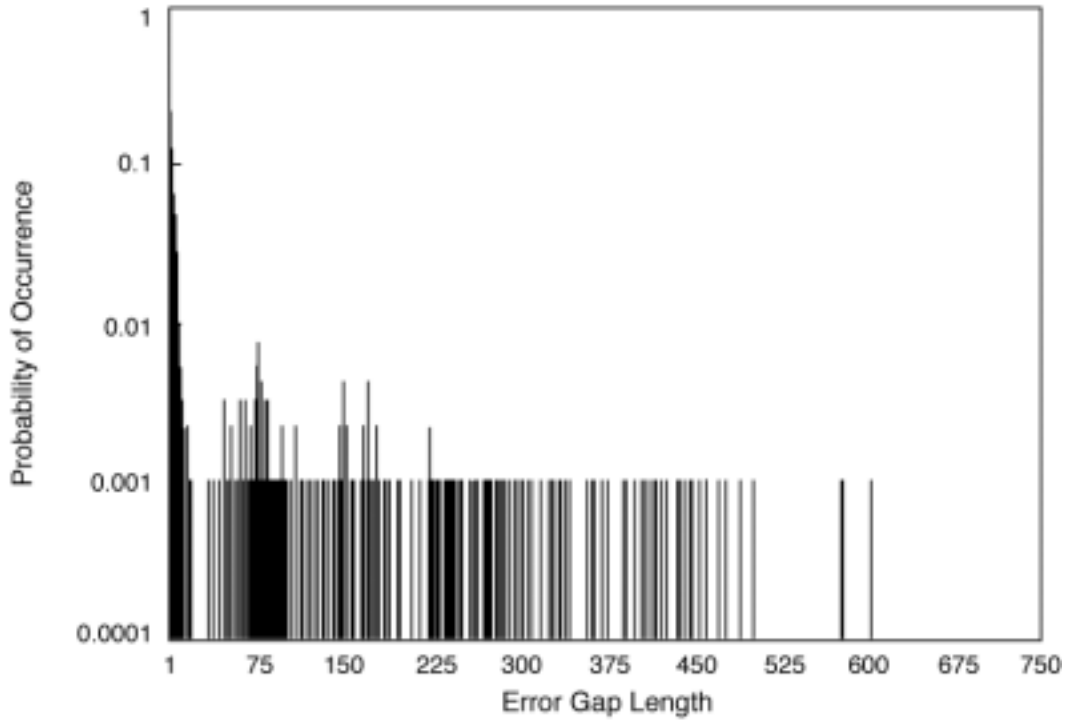


Figure 11. Comparison of error gap length distributions generated by (a) waveform simulation and (b) the Gilbert model for an IL land mobile radio link

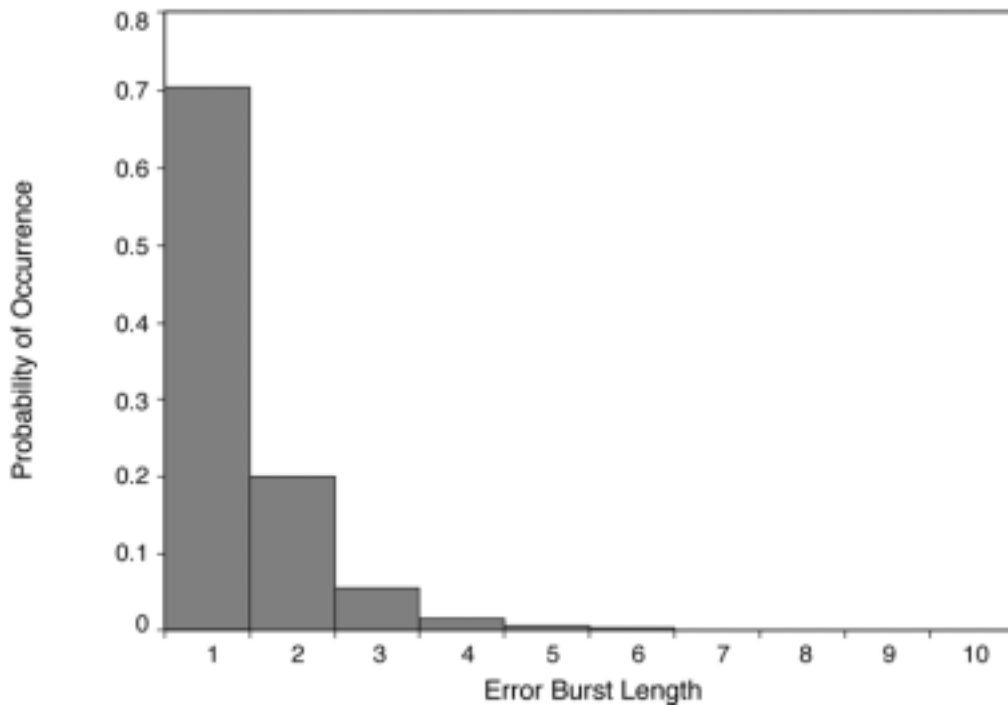
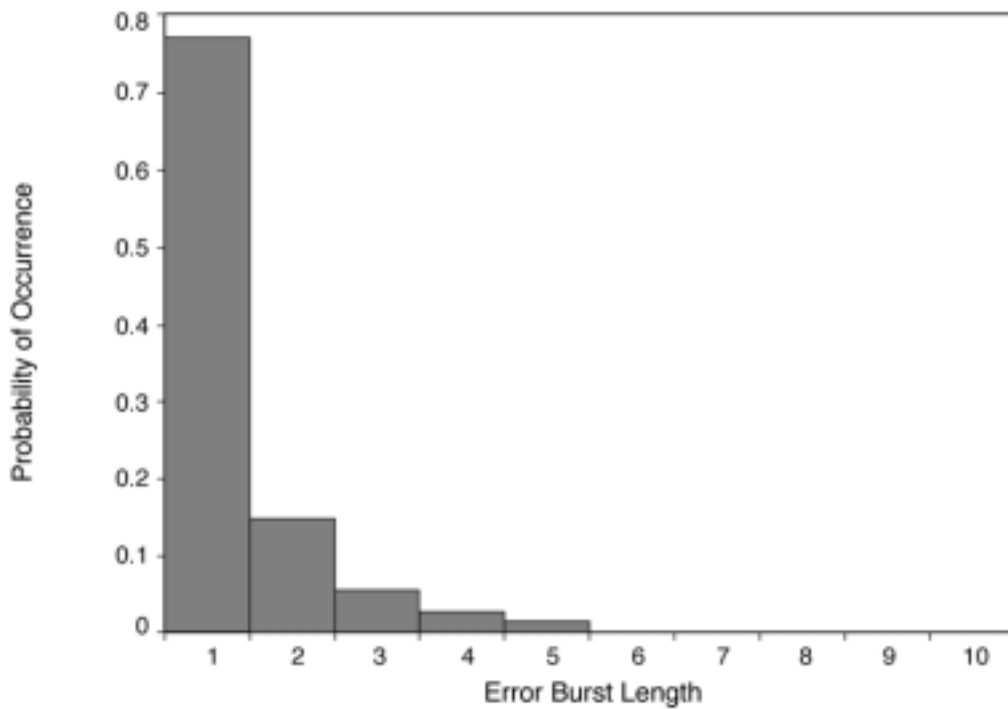


Figure 12. Comparison of error burst length distributions generated by (a) waveform simulation and (b) the Gilbert model for a NL land mobile radio link.

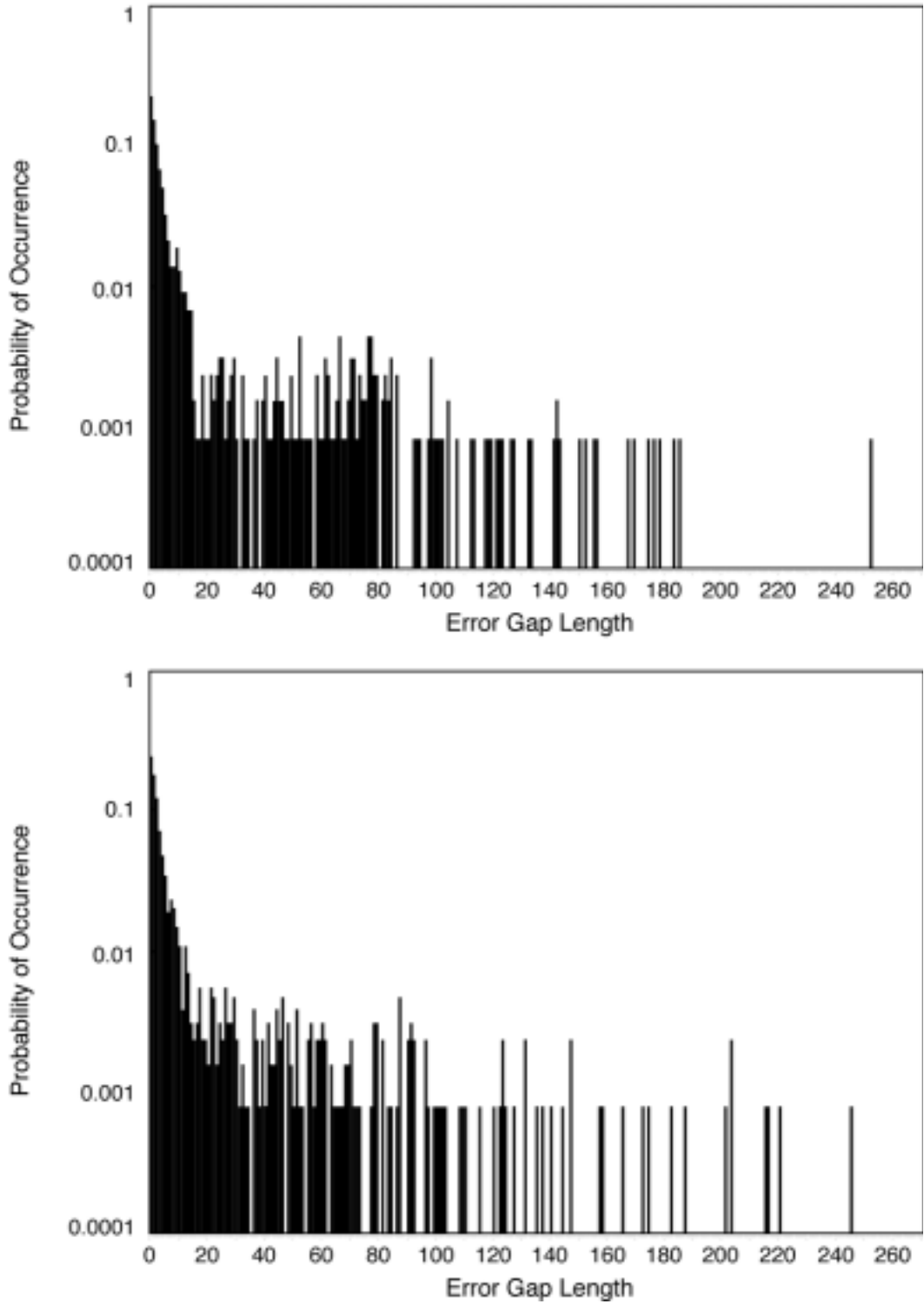


Figure 13. Comparison of error gap length distributions generated by (a) waveform simulation and (b) the Gilbert model for a NL land mobile radio link.

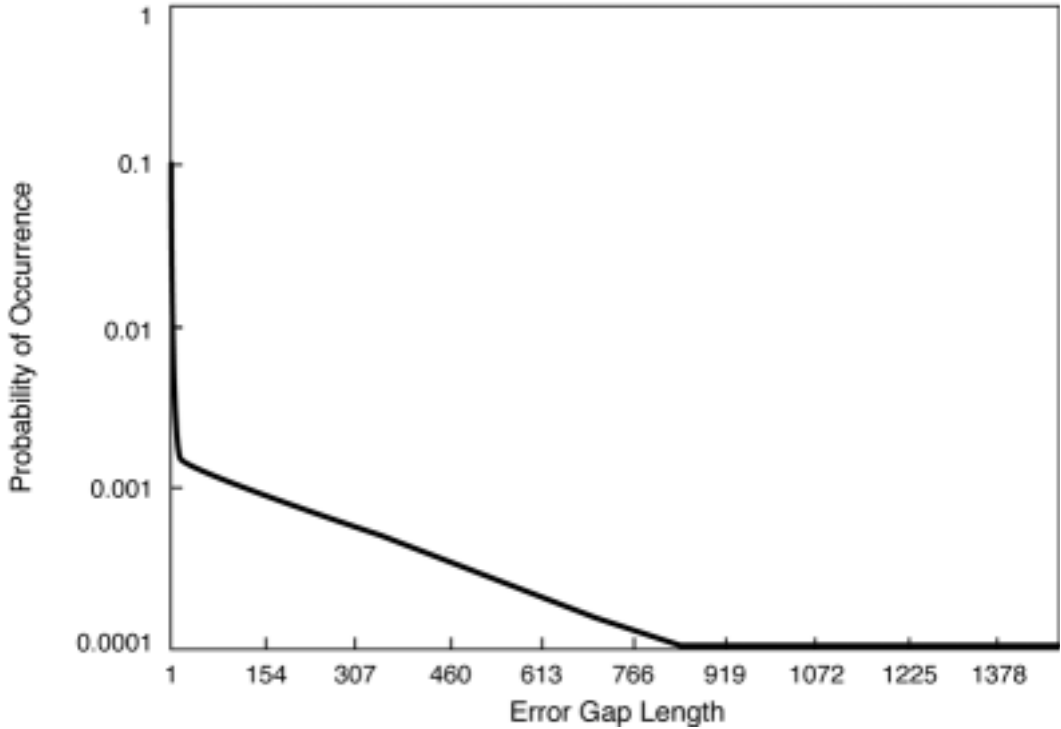


Figure 14. Plot of the analytic representation of the error gap length distribution in the Gilbert model for an “average” land mobile radio link.

6. WIRELESS LOCAL AREA NETWORK PERFORMANCE

To further investigate whether the Gilbert model can describe the error performance of wireless links, error processes generated by waveform simulations and by the model have been compared for a wireless local area network (WLAN). The WLAN uses an IEEE 802.11 proposed standard modulation, namely, frequency-hopped Gaussian minimum shift keying (GMSK). Multipath distortion was derived from impulse response measurements performed by ITS in an office environment at a center frequency of 1500 MHz [4]. Since the bandwidth of the channel measurements was considerably narrower than the 83.5 MHz hopping bandwidth of the proposed IEEE 802.11 standard, no hopping sequence was used in the simulations.

Direct sequence and frequency hopping modems will coexist in the same ISM band and are likely to generate cochannel interference to one another. Interference caused by a direct sequence modem was modeled as wideband noise and white Gaussian noise was also added to the distorted signal.

The signal source was an image derived from a standard bit map file obtained by scanning a U.S. Geological Survey topographic map. Pixel resolution was limited to 16 shades of gray represented by 4 bits.

Simulations were performed with a fixed carrier-to-interference ratio (CIR) of 10 dB and an SNR that varied from 0 to 28 dB in steps of 4 dB. Each simulation used 300,000 bits at a transmission rate of 1 Mbps. Details of the simulations, including the channel measurements, processing of the measured data, the GMSK modulation, and the modem architecture, have been discussed by Achatz and Qiuncy [5].

The error processes derived from the simulations were analyzed analogously to those for the land mobile radio links discussed in Section 5. The BER is plotted versus SNR in Figure 15. Error burst length and error gap length distributions were computed, and the means and variances of the distributions were used to determine values of q , Q , and h versus SNR. The results are shown in Figure 16. The dependencies of the parameters on SNR are qualitatively similar to those for the land mobile radio links at the corresponding power levels of signal, noise, and interference.

The values of the model parameters determined from the waveform simulations were then used in the model to generate error burst and error gap length distributions. The distributions closely resemble those generated by the waveform simulations. Example comparisons are shown in Figures 17 and 18 for an SNR of 12 dB. Note that these plots differ from those in Figures 6-13 for the land mobile radio links in that semi-log scales (rather than linear scales) and the analytical expressions for the model distributions (rather than simulated distributions) are used in the former. For these WLAN scenarios, the model runs approximately 15,000 times faster than the corresponding waveform simulations.

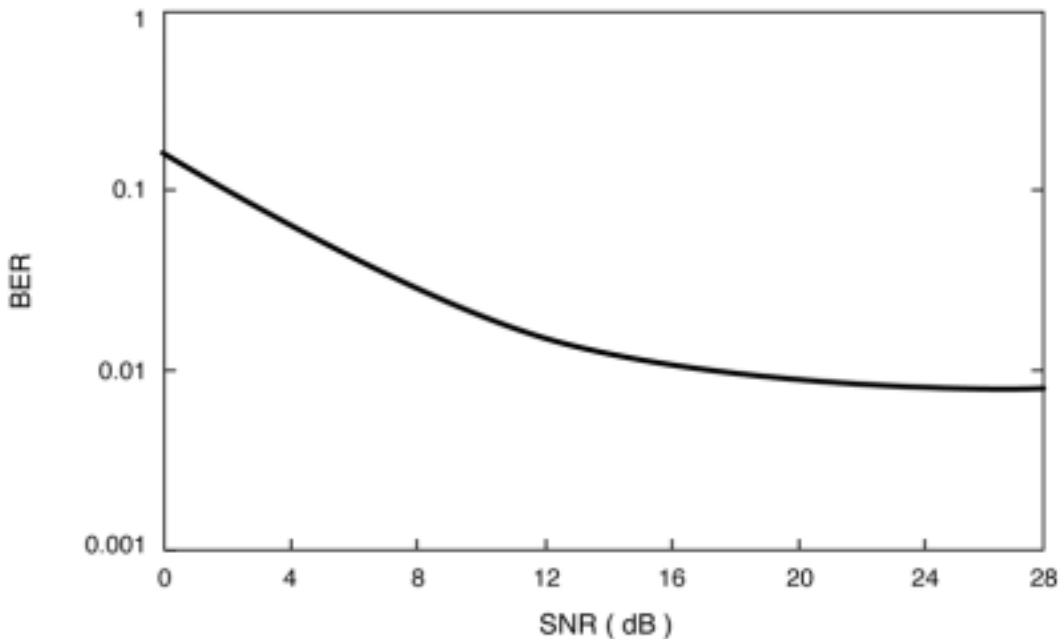


Figure 15. Wireless local area network performance relating BER to SNR.

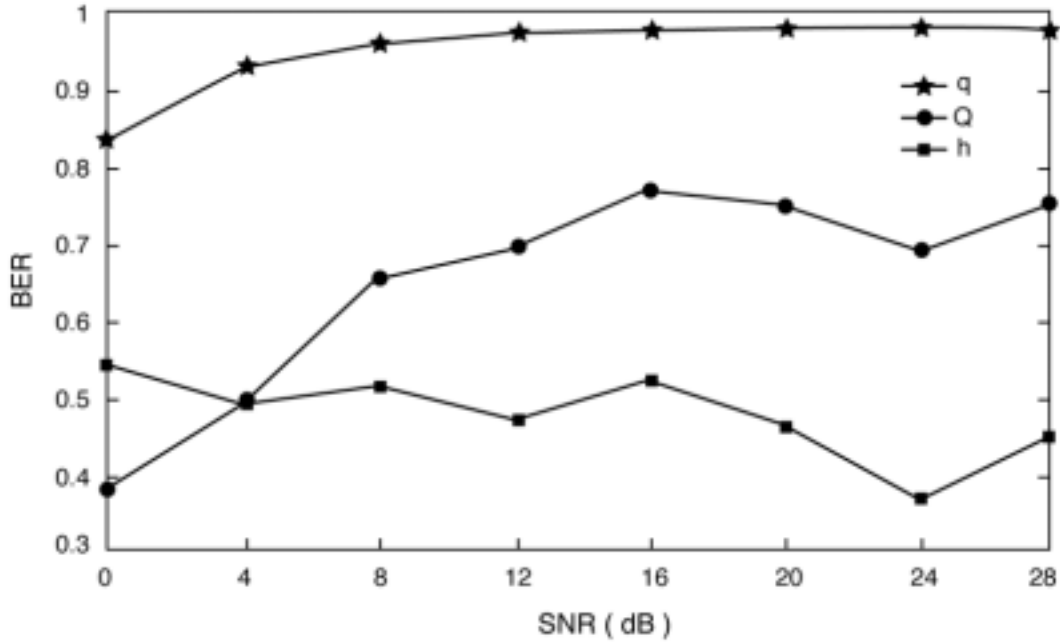


Figure 16. Gilbert model parameters q , Q , and h versus SNR for the wireless local area network link simulations.

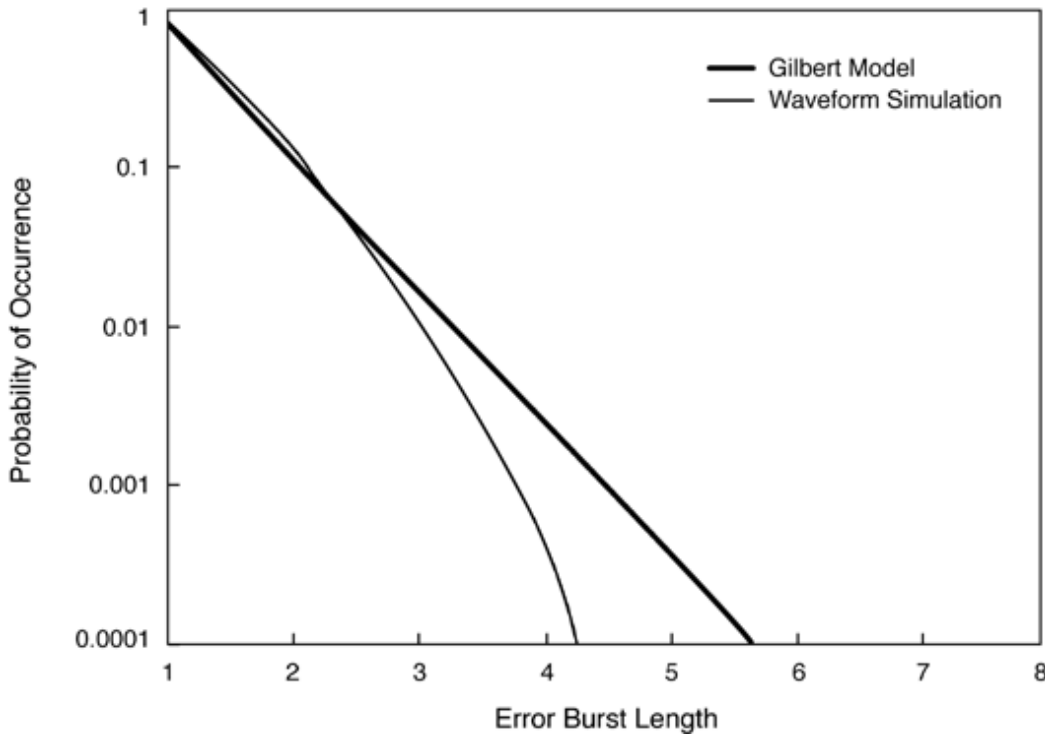


Figure 17. Error burst length distributions generated by a waveform simulation and by the Gilbert model for a wireless local area network with SNR = 12 dB and CIR = 10 dB.

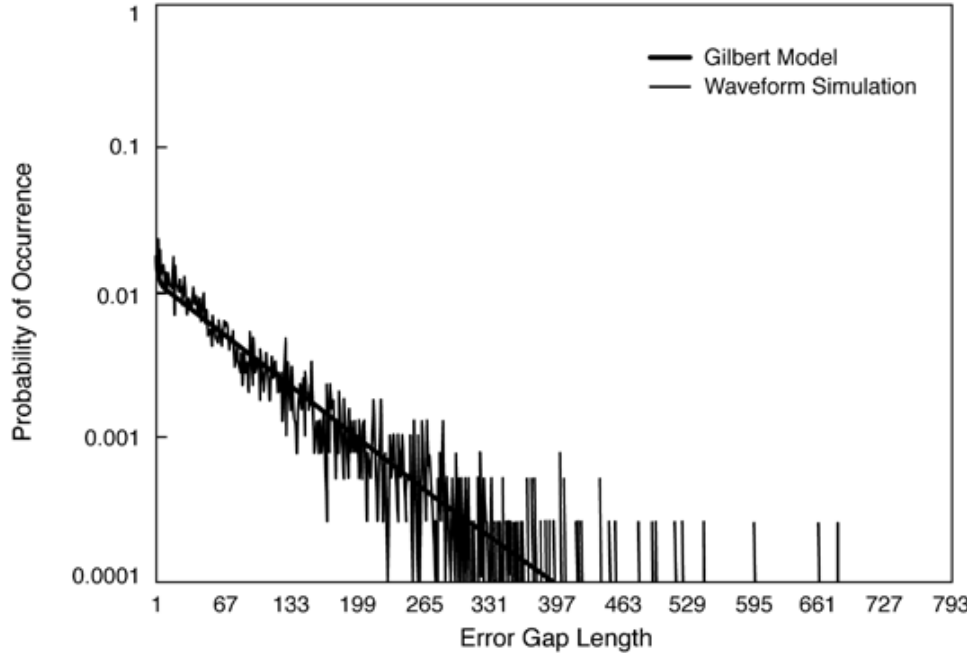


Figure 18. Error gap length distributions generated by a waveform simulation and by the Gilbert model for a wireless local area network with SNR = 12 dB and CIR = 10 dB.

7. CONCLUSIONS AND RECOMMENDATIONS FOR FURTHER WORK

The simple three-parameter model (Gilbert model) with parameter determination as described in this paper enables accurate simulation of the error processes for the wireless links that were investigated (land mobile radio and wireless local area networks). The error distributions derived from the model generally agree with those derived from waveform simulations.

The model is a powerful tool that can enhance network simulations and provide rapid evaluation of link quality. For the land mobile radio and local area network scenarios discussed in this work, the model runs faster than the corresponding waveform simulations by factors of approximately 50,000 and 15,000, respectively. As more elements are added to the link simulations (antennas, coding, etc.) these factors may increase considerably, due to the increased signal processing load in the waveform simulations. It is therefore recommended that this work be extended to other link conditions (propagation conditions, modulations, coding, antennas, etc.).

The model parameters appear to be well-defined, deterministic functions of the link conditions (signal-to-noise and signal-to-interference ratios). The dependence of the model parameters on link conditions could therefore be represented as functional relationships determined by empirical curve fitting. Such relationships would obviate the need to carry out additional waveform simulations or to carry out interpolations between previously determined values of the model parameters every time link conditions are varied.

8. ACKNOWLEDGMENTS

This work has been supported by the National Institute of Standards and Technology as part of the wireless communications performance benchmarking program. The author wishes to acknowledge E.A. Quincy for suggesting this problem and for helpful advice, R.J. Achatz for helpful discussions on discrete channel models and for assistance in carrying out the waveform simulations, and J.F. Mastrangelo for implementing the model and generating the numerical results presented in this report.

9. REFERENCES

- [1] E.N. Gilbert, "Capacity of a burst-noise channel," *Bell Syst. Tech. J.* 39, pp. 1253-1256, 1960.
- [2] E.A. Quincy and R.J. Achatz, "Wireless performance prediction via software simulation," in *Proc. of the IEEE Pac. Rim Conf. on Comm., Computers, and Signal Processing (PACRIM)*, Victoria, British Columbia, Canada, July 11-12, 1994.
- [3] D.C. Cox, "Distributions of multipath delay spread and average excess delay for 910 MHz urban mobile radio paths," *IEEE Trans. Ant. Prop.* AP-23, pp. 206-213, 1975.
- [4] P.B. Papazian, Y. Lo, E.E. Pol, M.P. Roadifer, T.G. Hoople, and R.J. Achatz, "Wideband propagation measurements for wireless indoor communications," NTIA Report 93-292, Jan. 1993.
- [5] R.J. Achatz and E.A. Quincy, "Performance prediction of WLAN speech and image transmission," in *Proceedings of the 1995 IEEE 45th Vehicular Technology Conference*, Vol. 2, Chicago, IL, Jul. 1995, pp. 559-563.